COMPUTATIONAL ANALYSIS OF URANYL SILICATES USING GAUSSIAN 98

A University Thesis Presented to the Faculty

of

California State University, Hayward

In Partial Fulfillment

of the Requirements for the Degree

Masters of Science in Chemistry

By

Veronica Wheaton

September, 2003

ABSTRACT

The structures of three uranyl silicate complexes were optimized and analyzed using the Gaussian98 computational program. Each complex contains a uranyl portion (UO_2) that is attached to a silicate base (SiO_2) to form a "bridged" complex. The monosilicate complex contained one silicate base, while the disilicate had two. There were two different bridged disilicate complexes to represent the symmetrical complex where the uranyl molecule is placed between two silicate bases and the unsymmetrical complex with the uranyl attached to a silicate base dimer. The purpose of this study is to investigate the complex formation between the uranyl ion and a silicate base structure, analyze the thermodynamic properties of each structure and the bonding nature of the various bonds within the complexes and compare them to experimental work, as well as to validate the concept of the "colloidal transport system".

COMPUTATIONAL ANALYSIS OF URANYL SILICATES USING GAUSSIAN 98

By

Veronica Wheaton

Approved:	Date:
Gregory Schenter	6/30/03
Michael Bowden	6/30/03
Jon Petersen	6/30/03

ACKNOWLEDGEMENTS

I would like to thank Dr. Leroy Chauffe for believing in my ability to maintain his standard of excellence in producing a top-notch thesis project. Also for introducing me to Dr. Balasubramanian whose affiliation with Lawrence Livermore National Laboratory enabled me to successfully complete the research for this thesis.

To my son, Jerrod Bolden, I hope and pray that watching mommy complete this thesis will provide the motivation for you to never give up and the challenge to reach farther than your eyes can see.

TABLE OF CONTENTS

LIST OF FIGURES

LIST OF TABLES

Chapter I - Introduction

The policy of the United States Government for the disposal of nuclear waste is to bury it in the ground and trust it doesn't leak out. Prior to the mid-1970's, U.S. utilities were to keep their spent fuel on-site then subsequently ship it to a reprocessing plant to recover the plutonium and uranium. However such a reprocessing plant was never developed. In 1982, the U.S. Congress passed the Nuclear Waste Policy Act which determined that stable geological formations be identified, i.e. Yucca Mountain Nevada, in which the spent nuclear fuel would be stored [1]. Consequently, studies to determine the migration behavior of actinide complexes have been conducted by a number of investigators.

Computational and experimental studies of actinide complexes are central to understanding the migration mechanisms of radionuclides from high-level radioactive wastes through the natural groundwater and soil. It is well known that the migrating actinide in the natural groundwater can be adsorbed onto geological interfaces (i.e. clay, minerals, etc.), plants and bacteria [2]. These environmental issues are of considerable interest because they involve the handling and disposal of radioactive wastes composed of various radionuclides.

It has been shown by extensive studies on the migration of Plutonium from waste storage facilities that the actinide can travel to locations over 200 miles away via the natural groundwater [2]. The transportation system investigated is termed the "naturally occurring mobile colloid system", which enhances the transport of the radionuclides through sorption [1]. The Nevada Testing Site was a prime location to

study due to the large amounts of radioactive materials located in the subsurface after underground testing. Plutonium was found in mineral colloid fractions of groundwater samples taken 1.3 km away from its original disposal site. Greater than 99% of the total Plutonium in the sample was associated with filtered colloidal materials composed of a mixture of clays, zeolites, and cristobalite [2]. These materials can be found in fractured volcanic rocks similar to those formed as a result of the fallout from testing. These minerals have a "high sorption capacity" for radionuclides, which makes them good transportation systems assuming the radionuclide was able to bind correctly and completely. The results of these studies proved conclusively that plutonium could exist as plutonium oxide, an intrinsic colloid, or could be adsorbed on a mineral surface to form a pseudocolloid; both of which have the ability to be transported by groundwater [2].

Uranyl silicate complexes are a part of a larger group of actinide complexes that has been analyzed, characterized, and synthesized over a period of time [2-6]. Experimentalists have looked into the binding nature of these complexes in search of patterns to explain their formation and degradation. Extended X-ray absorption fine structure analysis (EXAFS), multinuclear NMR, and Raman spectroscopy techniques have been used to analyze the thermodynamics of these actinide complexes [7-12].

Reich et al. [7] have carried out an Uranium L_{III} EXAFS study of U(VI) sorption onto silica gel as a function of U(VI) loadings at pH4. A fascinating outcome of this experiment is the discovery of two different sorption bridged complexes at different loadings. At higher loadings of 5- 70 mg U/g the EXAFS

spectra did not exhibit any U-Si interaction yet it possessed two types of U-O equatorial bonds, and the complex was termed a mononuclear inner sphere complex. But at lower U loadings of 0.5-1.0 mg U/g, the observed spectra seem to suggest the existence of a direct U-Si interaction along with a single, short U-O equatorial bond. This suggests a different bridged structure for the sorbed complex in which the uranyl (UO_2^{+2}) is bonded to a mono silicate in a bridged structure, that is, U binds to two of the oxygen atoms of the silicate in a bidentate complex. The missing U-Si bond at higher loadings suggests an entirely different structure, possibly a bridged structure involving more than one silicate. Moreover, the U-Si bond was found to be unusually short with a value of 2.72 A at 0.5 mg U/g. This value is shorter than any known U-Si bond in other U-Si minerals such as soddyite or uranophane, which exhibit U-Si distance of 3.16-3.17 A [7,8]. Thus there is a compelling need to carry out computations on these two types of uranyl silicate complexes to juxtapose the bonding features and to understand the unusually short U-Si bonding found in the EXAFS spectra at 0.5 mg U/g. Also included is the analysis of the bonding features and structural characteristics of such complexes to contrast the geometries and vibrational frequencies of the two bridged structures, and to provide unequivocal assignments of the observed EXAFS spectra at different loadings, which are not fully understood.

Gas-phase spectroscopic and theoretical studies of uranyl complexes have been the subject of many studies [13-16]. For example, Andrews and coworkers have studied IR spectra of matrix isolated uranyl species [9]. The uranyl molecule has

been studied using a variety of methods to understand its binding characteristics within the molecule as well as once a complex is formed [13,15,16].

Further investigation of the colloidal migration mechanism is needed to fully understand the phenomenon of actinide transport. The next logical step would be to research different naturally occurring mineral bases for their ability to bind actinides effectively. Majumdar and coworkers [18] used the carbonate molecule as the complex for binding to a uranyl structure, and found that very stable complexes could be computationally obtained and validated using the various experimental studies for comparison. Analyzing the various complexes formed between the uranyl molecule and the silicate structure, as a base will continue the investigation and validation of the "colloidal transport system".

Statement of the Problem

In this research project, we will calculate the optimized geometries of several uranyl silicate complexes in order to demonstrate the different ways a uranyl ion can bind to a silica interface or a colloid. Analysis of the computational results should reveal structures with different bonding and vibrational properties consistent with the Uranium L_{III} EXAFS work of Reich et al. [7]. The vibrational frequencies of the optimized structures are calculated to validate that the computed structures are true minima, and to compare the frequency data with EXAFS spectroscopic data. The nature of bonding in the uranyl silicate complexes along with the electronic charge distribution data will be analyzed to determine the stability of the U-Si bonds within the complex.

Chapter II - Methods and Models

Computational chemistry creates a model to which experimental data can be compared. This comparison provides validation of the model, enabling the researcher to expand the model to analyze other properties of a complex. The comparison of the computational data from various actinide studies [15,18] to known experimental work confirms the development of a quantum model that can be used for further analysis of actinide complexes.

Development of a valid model includes dealing with the challenges that come when computing the various thermodynamic properties of actinides. These challenges include the ninety-two protons in the uranium atom, the unpredictable electronic states of actinides, and the unpredictable nature of the 5f, 6d, and 7s orbitals that compete for binding. Previous computational models have tackled these challenges by taking into consideration the relativistic effects that affect actinides [17]. Relativistic effects are defined as "the differences in any measurable or observable properties that arise from the true velocity of light as opposed to the assumed infinite velocity" [17]. In using the *ab initio* computational method, the effective core potentials are handled by replacement of the core electrons with relativistic effective core potentials. This ignores the core electrons that are unimportant in the chemistry of the complex and leaves the valence electrons available for computational analysis.

The computational method that was used for this project was the Gaussian98 package of codes which is a system of programs connected together to perform the *ab initio* molecular orbital calculations. This method was chosen because it enabled a thorough calculation of the various thermodynamic properties for each complex, and was proven successful in a previous study of uranyl carbonates by Majumdar and coworkers [18].

Within the Gaussian98 series of programs there are a number of theories used for the optimization of the various geometries as well as for further validation of the results. We chose to use Density Functional Theory (DFT), which contained Becke's three-parameter functional [19] with Vosko et al's local correlation part [20], and Lee et al's non-local part [21] (abbreviated B3LYP). The DFT/B3LYP is used as an alternative to the conventional *ab initio* quantum mechanical methods, and is based on the Hohenberg-Kohn theorem that states, "energy and molecular properties are uniquely determined by the electron density" [22]. The second-order Moeller-Plesset Perturbation Theory (MP2) was used as a "higher level" calculation that would provide a more accurate account of the electronic structure for each of the complexes [22]. Since the MP2 method is computationally more intensive than the DFT/B3LYP theory, the results were considered more "correct". Both the DFT/B3LYP and MP2 theory level calculations were carried out using the Berny algorithm with redundant internal coordinates [23] to optimize the geometries and calculate the various thermodynamic properties of each complex.

To account for the relativistic effects on actinides, relativistic effective core potentials (RECPs) were used to replace the core electrons [24]. The valence Gaussian basis sets along with the effective core potentials were used during the computations to account for the unpredictable nature of the uranium 5f, 6d, and 7s orbitals that compete for binding. As in the uranyl carbonate study all calculations were carried out using RECPs that retained the outer $6s^2$ $6p^6$ 5f' $6d^1$ $7s^2$ shells of the uranium atom [25], and the corresponding optimized Gaussian basis set (5s 5p 4d 4f) contracted to 3s 3p 3d 2f was also used. The use of an extended basis set with an augmentation of the set of g polarization functions was not necessary since it showed no effect on the geometry optimizations in a previous study of uranyl carbonate complexes [18]. For the silicon and oxygen atoms, RECPs were used to retain the outer 2s and 2p shells in the valence space [26]. The corresponding basis sets for the silicate portion of the complex were taken from Pacios and Christiansen [26] and augmented with a six component 3d Gaussian function (0.85 for oxygen) as in the uranyl carbonate study.

The Posmol and Molten programs were used to interpret the calculated data from the Gaussian98 theories and provide an animated graphic of the vibrational frequencies and the various molecular orbital pictures for each uranyl silicate complex.

Three models were constructed based upon the proposed interactions of the uranyl ion with a surface similar to the optimized structures found in the carbonate

study [18]. Model 1 [Fig. 1] represents the interaction of the uranyl ion with a single silicate residue on the surface. Model 2 [Fig. 2] represents the uranyl ion interacting with two adjacent silicate residues on the surface, creating an "unsymmetrical" complex. Model 3 [Fig. 3] simulates the penetration of the uranyl ion into the top layer of the silicate surface, creating a "symmetrical" complex.

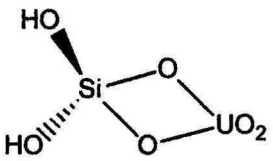

Figure 1

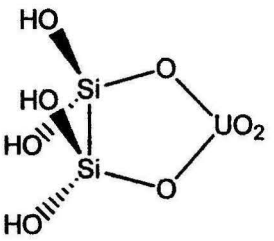

Figure 2

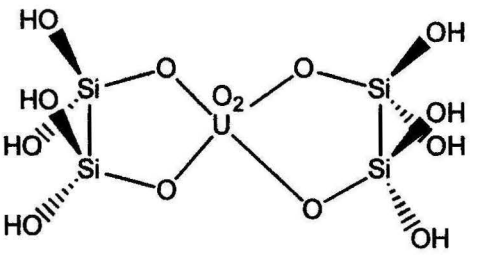

Figure 3

To create the proper geometry for each complex, a molecular model kit was used to construct the proposed complex structure and derive the correct coordinates for the z- matrix parameters. The z-matrix coordinates provide the input data for each of the proposed complexes from which the geometry can be optimized. The initial geometry is found from the RHF calculation of the z-matrix coordinates to find the complex minima. This geometry is then used as the input data for the DFT/B3LYP and MP2 calculations.

Chapter III - Results and Discussions

Equilibrium Geometries

The bonding nature of the uranyl ion, the silicate portion and the overall complex was analyzed using the optimized geometries calculated at both the DFT/B3LYP and MP2 theory levels. The bond lengths, bond angles, charge distribution data, and vibrational frequencies for each complex were analyzed to validate the initial geometries as true minima and not saddle points. The bond length and bond angle data were compared to the data from the uranyl carbonate study to show consistency in the computations [18]. This also validated that the proposed silicate complexes were optimized correctly. The charge distribution data, specifically the Mulliken Populations, enabled the quantitative analysis of the bonding between the uranyl portion and the silicate base. By animating the various vibrational frequencies for each complex, the type of vibrations within the complex could be compared to the IR spectral data of the uranyl orthosilicate experiment by Moll et al [10].

Uranyl monosilicate: The optimized structure of the uranyl monosilicate, Figure 4, shows the oxygens of the uranyl portion of the molecule are above and below the plane of U-Si ring as seen in the uranyl carbonate study [18], with the O-U-O bond angle approaching 180 degrees. This structure represents a bridged structure.

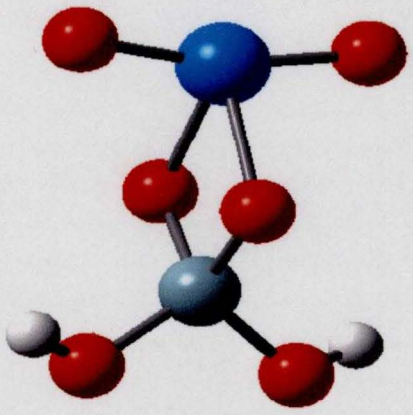

Figure 4: Blue ball represents uranium atom, red ball represents oxygen atom, grey ball represents silicon atom, and white ball represents hydrogen atom.

A list of the optimized bond distances and angles for the two levels of theory used in this study along with the available experimental data is shown in Table 1. The experimental data is from Demartin et al's study of uranyl orthosilicate hydrate by EXAFS. The distance between the uranium atom and the silicon atom is considered a "non-bonding" distance because they are not technically attached; however this distance is shorter than any known U-Si bond in other U-Si minerals such as soddyite or uranophane which exhibit U-Si distances of 3.16-3.17 [13]. Additionally, this shortened distance supports the bridged formation that the complex takes on. In comparing the two theory methods, the MP2 method calculated a shorter U—Si bond distance than the DFT/B3LYP method due to the accuracy with which the MP2 method can account for dispersive forces and other interactions that occur within the complex.

Table 1
Optimized Geometries of Uranyl Monosilicate

Geometric Parameters[a]	DFT/B3LYP	MP2	Experimental Data[b]
r(U-O)[c]	1.76	1.80	1.78
r(U-O)[d]	2.16	2.14	2.27
r(U—Si)	2.93	2.88	2.73
r(Si-O)[e]	1.69	1.70	1.64
r(Si-O)[f]	1.65	1.65	1.60
θ(O-U-O)	165.6	168.3	-
θ(O-U-O)	95.8	94.4	-
θ(O-Si-O)	112.9	112.4	-
θ(O-Si-O)	104.3	104.4	-

[a] The bond lengths(r) and angles (θ) are angstroms and degrees, respectively.

[b] F. Demartin et al Acta Crystallogr. C 48 (1992) 1.

[c] The U-O distance in the uranyl portion.

[d] Uranium connected to silicate oxygens.

[e] Silicon connected to the uranyl-binding oxygens.

[f] Si-O distance for hydroxy oxygens.

Unsymmetrical Uranyl Disilicate: The optimized structure of the unsymmetrical disilicate complex is shown in Figure 5. To achieve a truly stable disilicate complex, the initial geometry of the proposed Model 2 was modified manually via the input parameters. After setting fixed bond lengths and angles the Gaussian program could optimize the geometry and perform the same calculations as for the monosilicate complex. This "unsymmetrical" complex was created by fixing the dihedral angle connecting the uranyl portion to the silicate base (O=U-O-Si), and orienting the silicate base in the plane of the uranium atom. The bond lengths and bond angles were set to the fixed measurements calculated in the single-point geometry calculation, which maintained the configuration throughout the

optimization and enabled the same parameters to be calculated as in the monosilicate optimization.

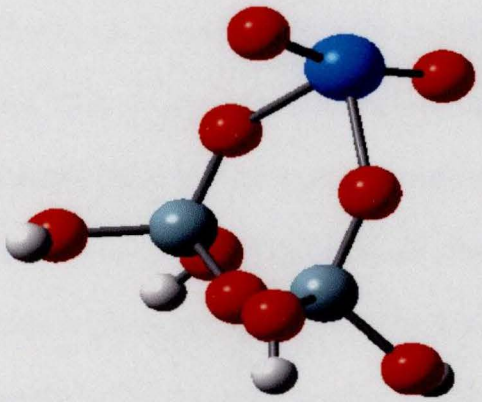

Figure 5: Blue ball represents uranium atom, red ball represents oxygen atom, grey ball represents silicon atom, and white ball represents hydrogen atom.

The uranyl portion came out much closer to linear due to the non-planar six-membered ring, and the positioning of the uranyl oxygen atoms above and below the plane. The six-member ring consisting of uranium, oxygens and silicon deviates from planarity by 5 degrees. Unlike the monosilicate complex, the uranium-silicate bond distance is too large to indicate any type of interaction between the two in the bridged structure (see Table 2). A larger charge transfer (see bonding analysis section) from the uranium atom to the equatorial oxygen atoms of the silicate base is indicated by the fact that these bonds are a bit shorter than in the monosilicate structure (2.12 vs 2.14, MP2 data).

Symmetrical Uranyl Disilicate: Attempts to optimize the structure of the symmetrical uranyl disilicate model did not give a minimum on the potential energy surface. A second or third degree saddle point resulted from each of our computation attempts. This could be due in part to the change in the coordination number on the uranium atom from a stable +6 to an unstable +8. As the Guassian program tried to optimize the proposed structure the size of the complex caused the calculation to be aborted. Most computational programs have difficulty calculating large complexes and therefore require a more sophisticated theory level for optimization. Due to the time constraints for this project, the symmetrical uranyl disilicate complex was omitted.

Table 2
Optimized Geometries of Unsymmetrical Uranyl Disilicate

Geometric Parameters[a]	DFT/B3LYP	MP2	Experimental Data[j]
R(U-O)[b]	1.76	1.79	1.78
R(U-O)[c]	2.14	2.12	2.27
R(U-Si)	3.58	3.54	2.73
R(Si-O)[d]	1.65	1.65	1.64
R(Si-O)[e]	1.67	1.67	-
R(Si-O)[f]	1.66	1.66	-
R(Si-O)[f]	1.66	1.65	1.60
R(Si-O)[f]	1.66	1.66	-
R(Si-O)[f]	1.66	1.66	-
$\theta(O_{ax}\text{-}U\text{-}O_{ax})$	166.1	169.3	-
$\theta(O_{ax}\text{-}U\text{-}O_{eq})$	95.5	94.4	-
θ(O-Si-O)[g]	107.2	107.1	-
θ(Si-O-Si)[h]	137.1	138.7	-
θ(O-Si-O)[I]	114.5	114.7	-
θ(O-Si-O)[I]	108.9	108.9	-
θ(O-Si-O)[I]	108.5	108.3	-
θ(O-Si-O)[I]	111.6	111.7	-

[a]The bond lengths (R) and bond angles (θ)are in angstroms and degrees respectively.

[b]The U-O distance in the uranyl portion.

[c]Uranium connected to silicate-binding oxygen.

[d]Uranium connected to the silicate oxygens.

[e]Silicate portions attached together by oxygen.

[f]Si-O distance for the unbound oxygen in the silicate portion.

[g]Angle between uranyl portion and silicate portion.

[h]Angle between two silicate portions.

[I]Angle between silicate portion binding oxygen and silicate terminal oxygens.

[j]Experimental results of hydrated uranyl orthosilicate crystal in solution from Ref. 13 (bridged structure).

Bonding Analysis

The molecular orbital coefficients were calculated for both the monosilicate and the "unsymmetrical" disilicate complexes. These calculations are used to indicate whether the type of bonding that occurs between the uranyl portion and the silicate base results in the overlap of the expected orbitals. Since the uranium atom's 5f, 6d, and 7s orbitals compete for binding, the proposed molecular orbitals should include both sigma (σ) and pi (π) overlap. The calculated coefficients can help to validate this theory showing that the π-type overlap occurs as a result of the uranium 5f atomic orbitals and the oxygen 2p atomic orbitals overlapping, and the σ-type overlap results when the uranium 6p atomic orbital overlaps the oxygen 2s atomic orbital.

The total charge on each atom in the uranyl monosilicate and disilicate complexes as inferred from the Mulliken populations is shown in Table 3. We also show the total charge on each component of both complexes. The charge distribution data for the monosilicate complex at the DFT/B3LYP level indicates that the uranyl portion has an overall charge of +0.63e, and the silicate portion has an overall charge of –0.63e. Upon formation of the uranyl silicate complex the charges cancel thus representing the formation of a stable neutral complex. Similar results were obtained from the MP2 data (UO_2 = +0.65e, SiO_2H_2 = -0.65e). A surface plot of the total SCF density of the monosilicate complex at an isosurface value of 0.08 is shown in Figure 6. The figure clearly shows the electron density from the uranium atom forming the bonds to the silicate oxygens.

Table 3 Calculated Mulliken populations for the Uranyl Monosilicate and Disilicate Complexes		
Atom	DFT/B3LYP (e)	MP2 (e)
Monosilicate Complex		
U	1.47	1.41
O	-0.417	-0.379
O	-0.418	-0.379
Si	2.16	2.26
O	-0.876	-0.910
O	-0.876	-0.910
O	-0.97	-1.02
O	-0.97	-1.02
H	0.449	0.473
H	0.449	0.473
UO_2 portion	0.632	0.652
SiO_4H_2 portion	-0.632	-0.654
Disilicate Complex		
U	1.62	1.63
O	-0.984	-1.04
Si	2.23	2.34
O	-0.369	-0.361
O	-0.369	-0.362
O	-1.17	-1.23
Si	2.23	2.34
O	-0.984	-1.04
O	-0.988	-1.04
O	-0.98	-1.03
O	-0.988	-1.04
O	-0.98	-1.03
H	0.445	0.469
H	0.445	0.469
H	0.445	0.469
H	0.445	0.469
UO_2 portion	0.832	0.907
$Si_2O_7H_4$ portion	-0.832	-0.894

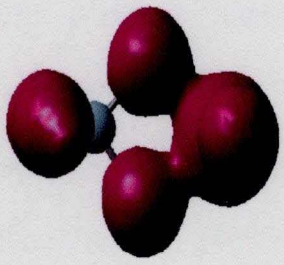

Figure 6

The Mulliken populations for the uranyl portion of the disilicate complex (+0.83e and +0.91e) for both the DFT/B3LYP and MP2 theory methods were equal and opposite those for the silicate base (-0.83e and –0.90e) validating the formation of a neutral complex, as in the case of the monosilicate. This also followed the trend found in the uranyl carbonate study [18] further validating the complex formation theory as well as the strength of the computational method used in the analysis. The analogous surface plot for the disilicate complex is shown in Figure 7.

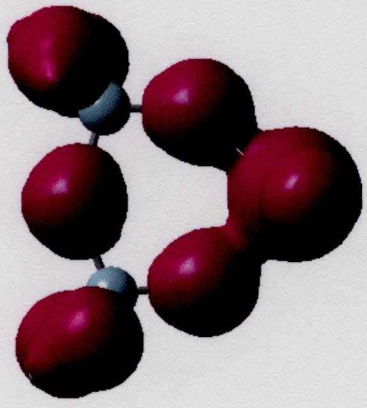

Figure 7

Molecular orbital coefficients were calculated at the MP2 theory level for both the monosilicate and disilicate uranyl complexes. Figure 8 shows the molecular orbital (MO) pictures of the highest occupied molecular orbital (HOMO), and the uranyl-silicate bonding orbitals. In the HOMO figures for both complexes, the uranium f orbitals are only involved in the uranyl (U-O) binding. This is consistent with the uranyl carbonate study by Majumdar et al [18].

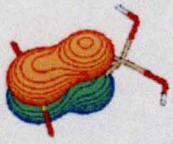

U-O-Si Bonding M.O.

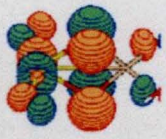

Uranyl M.O. (HOMO)

(a)

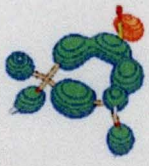

U-O-Si Bonding Orbital

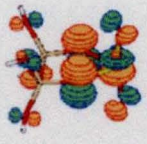

Uranyl M.O. (HOMO)

(b)

Figure 8

The HOMO compositions show that the uranium 6p and 5f orbitals are overlapping with the 2p orbitals of the silicate-binding oxygen atoms. This corresponds to π-type overlap between the 5f orbitals of the uranium atom and the 2p orbitals of the oxygens. As seen from Figure 8a, the uranyl-silicate overlap, the 6p orbital of the uranium atom overlaps with the 2s orbitals of the oxygen atoms, which is similar to σ-type bonding. The overlap features described above along with the Mulliken population values for uranium (1.47e for DFT/B3LYP and 1.41e for MP2) and oxygen (-0.417e for DFT/B3LYP and –0.379e for MP2) validate the strong molecular orbital binding for the complex. The transfer of electrons between the uranyl portion and silicate base assists the bonding.

The uranyl-silicate orbitals are also represented in Figure 8b. The 3s orbitals contribute to the bonding by overlapping with the 2s orbitals of the oxygen atoms of the silicate base. As shown in Figure 8b, the bonding of the uranyl portion to the silicate base is strengthened due to the exchange of electrons from the uranium atom through the silicate oxygen. Similar to the monosilicate case in Figure 8a, the Mulliken population values for the uranium (1.62e for DFT/B3LYP and 1.63e for MP2) and oxygen (-0.396e for DFT/B3LYP and –0.362e for MP2) show that there is also charge delocalization in the disilicate complex.

An important result from the analysis of the bonding in the uranyl complexes is obtained when one considers our findings in light of the work of Reich et al [7]. They concluded from the Uranium L_{III} EXAFS analysis of uranium sorbed onto silica gel that two possible structures are formed. Their study showed that the

structure formed at low uranium loading (0.5-1 mg U/g) is quite different from the structure obtained at high uranium loading (5-70 mg U/g). The EXAFS spectra suggested a structure with unusual U-Si interaction due to the short U-Si distance of 2.73 Å. They concluded there was no U-Si interaction at uranium loading above 1 mg U/g.

On the basis of the experimental U-Si distance of 2.73 and the observed U-O_{ax} and U-O_{eq} distances of 1.78 Å and 2.27Å respectively, we can assign the structure observed at the lower loading to uranyl monosilicate, Figure 4. At the higher uranium loading, the observed structure should closely relate to the bridged disilicate, Figure 5, which does not exhibit any U-Si bonding. The only inconsistency to these assignments is that the EXAFS spectra suggest the possibility of two non-equivalent equatorial oxygens at the higher uranium loading while our computed optimized structure exhibits equivalent U-O_{eq} bonds.

Spectral Analysis

Vibrational frequencies are calculated in this study to show that the optimized structures in Figure 4 and Figure 5 are true minima, and to validate the results with experimental vibrational frequencies on related species. True minima are established when an "imaginary" frequency is calculated for the optimized structure. The vibrational frequencies of the complexes at both levels of theory are shown in Table 4.

Table 4 Vibrational Frequencies at Both Levels of Theory		
Molecule Name	Method	Frequencies, cm^{-1} (IR Intensities)
$UO_2SiO_4H_2$	DFT/B3LYP	73(0.15), 89(1.04), 152(2.40), 184(6.02), 206(0.06), 218(1.03), 247(162.50), 251(155.46), 264(23.42), 299(0.43), 370(5.62), 379(81.18), 503(99.23), 609(265.64), 701(10.71), 722(150.57), 829(281.46), 859(129.96), 902(9.96), 937(360.76), 948(673.03), 990(56.12), 3864(1.92), 3865(119.06)
$UO_2SiO_4H_2$	MP2	64(0.10), 91(1.06), 176(5.33), 198(3.13), 203(10.06), 242(18.47), 248(103.59), 259(109.38), 310(1.33), 385(83.39), 510(95.78), 608(323.95), 702(54.67), 725(195.57), 847(88.03), 850(289.60), 910(92.89), 914(325.47), 968(660.78), 1011(25.50), 3908(1.71), 3910(157.41)
$UO_2Si_2O_7H_4$	DFT/B3LYP	32(1.99), 33(0.38), 43(5.77), 126(107.38), 132(14.80), 149(1.02), 167(25.87), 170(8.67), 185(0.55), 193(58.30), 217(34.92), 222(35.73), 230(28.74), 231(7.13), 263(63.13), 271(7.55), 303(100.60), 318(18.52), 349(143), 356(3.06), 414(93.94), 424(0.33), 486(52.48), 501(174.80), 659(129.59), 758(28.87), 828(21.60), 830(222.95), 844(470.52), 852(492.95), 858(0.64), 922(134.81), 935(312.90), 948(404.11), 970(222.92), 980(0.16), 1005(648.35), 1007(589.35), 3857(90.77)

In comparing the vibrational frequencies computed in this study with those of the carbonate [18], similar results are noted. The symmetrical stretching modes for the uranyl portion of the monosilicate complex at DFT/B3LYP and MP2 levels of theory were 859 and 847 cm^{-1}, respectively. These values varied little from those obtained in the carbonate study and therefore agree with previous experimental data.

The asymmetric stretching modes (DFT/B3LYP = 937 cm^{-1}; MP2 = 914 cm^{-1}) follow the same trend.

Using various software packages to visualize the frequency data shown in table 4 for the disilicate complex, two mixed-mode frequencies were observed at 659 cm^{-1} and 828 cm^{-1} at the DFT/B3LYP theory level. The term "mixed-mode" refers to two distinct modes being observed at one frequency. Being a larger complex, the expected result would be an increase in the amount of motion at a variety of frequencies, which was observed at these frequencies. At the higher frequency (828 cm^{-1}), the Si-O bond showed asymmetric stretching with a U-O twisting occurring simultaneously. At 844 cm^{-1} both the uranyl U-O bond and the silicate Si-O bond showed asymmetric stretching. In the mono silicate complex, only one vibrational mode in the DFT/B3LYP and MP2 theories corresponds to the stretching of the silicate portion of the complex as well as bending of the uranyl portion. The U-Si-O stretching and O-U-O bending modes can be found clearly at 701 cm^{-1} and 702 cm^{-1} for the DFT/B3LYP and MP2 theory levels, respectively. This is observed visually when the complex is rotated so that the portion of the complex lying in the xy plane is where the uranyl binds to the silicate, positioning the uranyl oxygens above and below the plane.

The computed vibrational frequencies for the uranyl monosilicate (Figure 4) are in very good agreement with the observed IR spectra of uranyl orthosilicate by Moll et al [10], when comparing observed bands with the computed results reported

in Table 4. The computed U-O_{ax} asymmetric stretching frequency is 937 cm^{-1} and 914 cm^{-1} at the DFT/B3LYP and MP2 levels, respectively, compared to Moll et al.'s value of 920 cm^{-1}. The axial U-O_{ax} symmetric stretch frequency of 859 cm^{-1} and 847 cm^{-1}, at the DFT and MP2 levels, respectively, compared to the IR absorption value of 835 cm^{-1}. The bending mode frequency for UO_2 as 264 cm^{-1} and 259 cm^{-1}, at DFT and MP2 levels, respectively, compared to 278 cm^{-1} obtained by Moll et al.

The computed vibrational modes involving Si-O stretching and bending mixed with the U-O_{eq} motions agrees quite well with the experimental data of Moll et al. However, there is a difference in how these various modes are assigned, due to the fact that computed data shows considerable mixing with equatorial U-O motions versus experimental data that attributes these modes to pure SiO_4 modes.

Experimentally, Moll et al. assigned a vibrational frequency of 963 cm^{-1} to a SiO_4 stretch mode. Computationally the frequency values of 948 cm^{-1} and 968 cm^{-1} for the DFT/B3LYP and MP2 theories, respectively, corresponded to a mixture of SiO_4 stretching and -OH bending when animated. At 609 cm^{-1} and 608 cm^{-1} (for DFT/B3LYP and MP2) the first bending mode combined with an U-O_{eq} symmetric stretch was observed which corresponded to the experimental value of 617 cm^{-1}, the pure SiO_4 bending mode according to Moll et al. A second mode corresponding to the experimental result of 520 cm^{-1} was calculated at 503 cm^{-1} and 510 cm^{-1}, for the DFT/B3LYP and MP2 theories, respectively. This mode was a combination of the U-O_{eq} asymmetric stretching and Si-O bonds connected to the uranyl bending.

The rocking of the silicate in combination with the bending of the U-O_{eq} bonds occurred at a value of 299 cm^{-1} (DFT/B3LYP) and 310 cm^{-1} (MP2). Moll et al. observed experimentally that a frequency value of 315 cm^{-1} only corresponded to the bending of the SiO_4 portion of the complex.

The unobserved low frequency bending involving both axial and equatorial atoms attached to U occurs at 184 cm^{-1}, but it is unlikely to be observed due to its low IR intensity. This mode corresponds to concerted rocking of the UO_2 axial atoms and the silicate without much change in the bond distances. The mode at 379 cm^{-1} (DFT) and 385 cm^{-1} (MP2) is most probably akin to the unobserved modes at 420- 431 cm^{-1} involving a concerted rocking of the molecule without much change to the U-O or Si-O distances. A primary difference between this and the mode at 184 cm^{-1} is that this mode involves concerted rocking motion of the equatorial oxygen atoms and the oxygen atoms attached to Si. Whereas the mode at 184 cm^{-1} involves uranyl axial oxygen atoms and the silicate O atoms not bonded to U. Finally, the computed O-H stretching frequency is 3865 cm^{-1} and 3910 cm^{-1} compared to 3450 cm^{-1} observed for the orthosilicate.

Thermochemistry

We thought it would it would be informative to compare the enthalpies of formation of uranyl monosilicate with the unsymmetrical uranyl disilicate. If one can assume that solvation effects for the two complexes would be comparable then a

comparison of the enthalpies of formation in the gas state should be valid. Table 5 shows the data used in the calculations. The ΔH_{corr} is the correction factor for each of the enthalpy values as read directly from the output file. The calculations were completed and the final enthalpy units converted from Hartrees to kcal/mol.

(1) $UO_2^{+2} + SiO_4H_2^{-2} = UO_2SiO_4H_2$

(2) $UO_2^{+2} + Si_2O_7H_4^{-2} = UO_2Si_2O_7H_4$

Table 5 (Enthalpies in Hartrees)

Molecule	ΔH	ΔH_{corr}
UO_2^{+2}	-82.842471	0.009737
$SiO_4H_2^{-2}$	-69.005623	0.041097
$Si_2O_7H_4^{-2}$	-122.288408	0.083199
$UO_2SiO_4H_2$	-152.878477	0.053133
$UO_2Si_2O_7H_4$	-206.093330	0.093837

$\Delta H(UO_2SiO_4H_2) = -613.38$ kcal/mol

$\Delta H(UO_2Si_2O_7H_4) = -603.38$ kcal/mol

These data show that the monosilicate complex is 10 kcal/mol more stable than the disilicate. Assuming that the more stable product is thermodynamically favored then the monosilicate probably forms faster than the disilicate. These results are consistent with the assignments of the two structures based on Reich's [7] uranium loading study.

Chapter IV – Summary

Understanding the mechanism of how heavy metals from nuclear waste might migrate from their buried disposal sites is an important issue of environmental concern. The low solubility of the actinides, such as uranium, can be offset by their ability to form soluble colloids with minerals present in the disposal pits. Insight into these naturally occurring mobile systems is vital. This study of the interaction of uranium with silicates deals with these issues.

Our study used the Gaussian98 package of computational codes. The investigation of probable uranyl – silicate interactions yielded two stable complexes. The optimized structures of the two complexes, uranyl monosilicate, Figure 4, and uranyl disilicate, Figure 5, were shown to be true minima from the frequency calculations. Structural features of these complexes were compared with those features of the analogous uranyl carbonate study by Majumdar [18] and the results were very consistent. Both optimized structures had bridged geometries with the monosilicate exhibiting extra stability through an unusually short U-Si bond not observed in the disilicate. Calculation of the enthalpies of formation for the two complexes showed that the monosilicate was 10 kcal/mol more stable than the disilicate. These data explain the experimental results of Reich [7]. His Uranium L_{III} EXAFS spectral analysis of uranyl sorbed on silica gel indicated the presence of two different species at different uranium loadings.

Our computational analysis provided confirmation of the assignment of the observed structure at low uranium loading (0.1-0.5 mg U/g) to uranyl monosilicate, Figure 4, and the structure at higher loadings to the disilicate, Figure 5.

The observed IR spectrum of uranyl orthosilicate was assigned to the corresponding vibrational frequency calculation. Overall the computed MP2 frequencies of uranyl monosilicate were in good agreement with those observed experimentally by Moll et al. [10]. However, by animating the corresponding vibrational frequencies, we were forced to reassign some of the modes attributed to pure silicate modes in Moll's work to a combination of linked uranyl and silicate modes.

This study also provided insight into the types of bonding taking place within each complex through the use of the Mulliken Populations, molecular orbital and charge transfer calculations. Consistent with the bonding features found in the uranyl carbonate study, the uranyl silicate complexes exhibit U(5f) – O(2p) π-overlapping. Thus the predicted bonding nature of the uranyl ion (UO_2^{+2}) to a silicate (SO_4) colloid, as well as to the sorption complex on silica gel was validated.

REFERENCES

[1] D.L. Clark, Los Alamos Science, Number 26 (2000).

[2] A.B. Kersting, D.W. Efurd, D.L. Finnegan, D.J. Rokop, D.K. Smith, and J.L.Thompson, Nature 397 (1999) 56.

[3] C.A. Blake, C.F. Coleman, K.B. Brown, D.G. Hill, R.S. Lowrie, and J.M. Schmitt, Journal American Chemical Society 78 (1956) 5978.

[4] V.I. Paramonova, B.P. Nikolskii, N.M. Nikolaeva, and J. Russ, Inorganic Chemistry 7 (1962) 528.

[5] E.T.Strom, D.E. Woessner, and W.B. Smith, Journal American Chemical Society 130 (1981) 1255.

[6] P.G. Allen, J.J. Bucher, D.L. Clark, N.M. Edelstein, S.A. Ekberg, J.W. Gohdes, E.A. Hudson, N. Kaltsoyannis, W.W. Luken, M.P. Neu, P.D. Palmer, T. Reich, D.K. Shuh, C.D. Tait, and B.D. Zwick, Inorganic Chemistry 34 (1995) 4798.

[7] T. Reich, H. Moll, T. Arnold, M.A. Denecke, C. Hennig, G. Geipel, G. Bernhard, H. Nitsche, P.G. Allen, J.J. Bucher, N.M. Edelstein, and D.K. Shuh, Journal Electron Microscopy and Related Phenomenon 96 (1998) 237.

[8] T. Reich, H. Moll, M.A. Denecke, G. Geipel, G. Bernhard, H. Nitsche, P.G. Allen, J.J. Bucher, N. Kaltsoyannis, N.M. Edelstein, and D.K. Shuh, Radiochimica Acta 74 (1996) 219.

[9] L. Andrews, M. Zhou, B. Liang, J. Li, and B.E. Bursten, Journal American Chemical Society 122, Number 46 (2000) 11440.

[10] H. Moll, W. Matz, G. Schuster, E. Brendler, G. Bernhard, and H. Nitsche, Journal Nuclear Materials 227 (1995) 40.

[11] D.C. Koningsberger and R. Prins, "X-Ray Absorption. Principles, Applications, and Techniques of EXAFS, SEXAFS, and XANES", John Wiley and Sons, Inc., New York, 1988.

[12] E.L. Belokoneva, V.I. Mokeeva, L.M. Kutznetsov, M.A. Simonov, E.S. Marakov, and N.V. Belov, Dokl. Akad. Navk SSSR 246 (1979) 93.

[13] F. Demartin, C.M. Gramaccioli, and T. Pilati, Acta Crystallogr. C48 (1992) 1.

[14] Z. Zhang and R.M. Pitzer, Journal Physical Chemistry A 103 (1999) 6880.

[15] J. Li, B.E. Bursten, B. Liang, and L. Andrews, Science 295 (2002) 2242.

[16] M. Boring, J.H. Wood, and J.W. Moskowitz, Chemical Physics 63, Number 2 (1975) 638.

[17] K. Balasubramanian, "Relativistic Effects in Chemistry: Parts A & B", Wiley Interscience New York, NY 1997.

[18] D. Majumdar, K. Balasubramanian, and H. Nitsche, Chemical Physics Letters 262 (2002) 143.

[19] A.D. Becke, Journal Chemical Physics 98 (1993) 5648.

[20] S.H. Vosko, L. Wilk, and M. Nusiar, Canadian Journal Physics 58 (1980) 1200.

[21] C. Lee, W. Yang, and R.G. Parr, Physics Review B37 (1988) 785.

[22] P.V.R. Schleyer, Encyclopedia of Computational Chemistry 3 (1998) 1706.

[23] C. Peng, P.Y. Ayala, H.B. Schelegel, M.J. Frisch, Journal Computational Chemistry 17 (1996) 49.

[24] P.V.R. Schleyer, Encyclopedia of Computational Chemistry 4 (1998) 2471.

[25] W.C. Ermler, R.B. Ross, and P.A. Christiansen, International Journal Quantum Chemistry 40 (1991) 829.

[26] L.F. Pacios and P. A. Christiansen, Journal Chemical Physics 82 (1985) 2664.

APPENDIX

A. Sample Input File: Optimization and Frequency Calculation of Uranyl Monosilicate

B. Sample Output File (partial): Optimization of Uranyl Cation

Sample A

```
%mem=300mb
%chk=d:\veronicasummer\uo2sio4h2_dft1_opt.chk
%rwf=1,245mw,2,245mw,3,245mw
#P b3lyp/gen 5d,7f pseudo=read gfprint scf=(direct,maxcyc=600)
opt=(redundant,maxcyc=600)freq geom=modify guess=read

  UO2SiO4H2 + DFT Optimization Calulation

 0  1

d 7 4 8 9 120.0 a

 U 0
S 1 1.0
0.9978 -2.268898
S 1 1.0
0.7281  2.684396
S 1 1.0
0.2132  0.447389
S 1 1.0
0.1092 1.0
S 1 1.0
0.0346  1.0
P 3 1.0
1.4248  -0.312884
0.6453  0.664164
0.2711  0.543576
P 1 1.0
0.1019  1.0
P 1 1.0
0.0308  1.0
D 2 1.0
2.1505  -0.016826
0.3844  0.392433
D 1 1.0
0.1419 1.0
D 1 1.0
0.0492 1.0
F 3 1.0
4.3777  0.190893
1.7970  0.452772
0.7050 0.436897
F 1 1.0
0.2425  1.0
 ****
 O   0
 S   2  1.00
          8.65700000        -0.13299000
          0.86920000         0.56168600
 S   1  1.00
```

```
          0.39940000          1.00000000
 S    1  1.00
          0.19780000          1.00000000
 P    2  1.00
          13.3400000          0.06263200
           3.01600000         0.28032600
 P    1  1.00
          0.84890000          1.00000000
 P    1  1.00
          0.23710000          1.00000000
 D    1  1.00
          0.85000             1.00000000
 ****
 Si   0
 S    2  1.00
          11.0700000          1.00000000
           1.22100000         1.00000000
 S    1  1.00
          0.24730000          1.00000000
 S    1  1.00
          0.86240000          1.00000000
 P    1  1.00
          6.67100000          1.00000000
 P    1  1.00
          2.12000000          1.00000000
 P    1  1.00
          0.29750000          1.00000000
 P    1  1.00
          0.88670000          1.00000000
****
 H    0
 S    1  1.00
          13.3600000          1.00000000
 S    1  1.00
          2.01300000          1.00000000
 S    1  1.00
          0.45380000          1.00000000
 S    1  1.00
          0.12330000          1.00000000
*********

U 0
U-ECP 4 78
G Potential
7
2  1.2229  -0.951647
2  2.6710  -10.774639
2  6.1090  -33.548874
2  17.9193  -122.391617
2  49.8812  -256.048798
2  169.5519  -721.334717
1  605.9017  -75.180313
S-G Potential
```

```
9
2  2.0820  86.946999
2  2.3616  -324.482452
2  3.0496  754.809631
2  4.2889  -931.611450
2  6.3681  867.389343
2  9.7364  -567.786743
2  15.3593  467.569519
1  43.8521  87.235092
0  131.5121  6.009224
P-G Potential
9
2  1.5561  109.529152
2  1.7721  -372.342407
2  2.2584  760.677795
2  3.0945  -945.122620
2  4.5103  906.449463
2  6.7113  -618.621948
2  10.0177  434.298340
1  28.2983  96.911469
0  89.1060  8.633708
D-G Potential
9
2  1.0371  98.695557
2  1.1784  -348.774384
2  1.4458  647.684631
2  1.9168  -796.751953
2  2.6533  775.700195
2  3.7460  -576.682800
2  5.0372  328.078552
1  15.9288  70.240524
0  48.0590  7.229150
F-G Potential
9
2  0.9036  -0.776395
2  2.8469  64.140816
2  3.6708  -301.194977
2  4.8940  617.674927
2  7.3913  -840.648010
2  11.6596  1010.848450
2  18.2575  -503.985931
1  28.9229  116.525749
0  137.5646  8.050508
O   0
O-ECP    1    2
P POTENTIAL
 3
2          10.02860000        -0.79842000
2          34.19800000        -5.76684700
1         100.00390000        -1.48645600
S-P POTENTIAL
 4
2           2.24790000        11.21630400
```

```
2           2.40490000      -16.34447700
1           4.37400000        1.04294400
0           2.18920000        2.19389100
SI   0
SI-ECP    2    10
D POTENTIAL
 4
2           1.62109999       -0.67587200
2           4.53210002       -6.72859800
2          13.20760000      -19.62386489
1          39.96990013       -6.58675301
S-D POTENTIAL
 5
2           1.86890000      -54.56442690
2           2.11390001      146.37274933
2           2.45269999      -88.33109474
1           3.88029999        6.76354098
0           2.56439999        3.11288401
P-D POTENTIAL
 5
2           2.47999999      116.56166363
2           2.97729999     -224.59841347
2           3.77399999      138.22863007
1           5.56639999        2.85250399
0          10.31330001        5.07075799
```

Sample B

```
*****************************************
Gaussian 98:  x86-Win32-G98RevA.9 19-Apr-2000
                 03-Mar-2003
*****************************************
%mem=8MW
%chk=UO2_ion2.chk
----------------------------------------------------------------------
# b3lyp/gen 5d,7f pseudo=read nosymm scf=(maxcyc=600) opt=(CalcFC,redu
ndant,maxcyc=100) geom=connectivity
----------------------------------------------------------------------
1/6=100,10=4,14=-1,18=20,26=3,38=1,57=2/1,3;
2/9=110,15=1,17=6,18=5,40=1/2;
3/5=7,8=11,11=2,16=1,17=8,25=1,30=1/1,2,3;
4/11=1/1;
5/5=2,7=600,38=4,42=-5/2;
8/6=4,11=11/1;
11/6=1,8=1,9=11,15=111,16=11,31=1/1,2,10;
10/6=1,7=6,31=1/2;
6/7=2,8=2,9=2,10=2,28=1/1;
7/10=1,18=20,25=1,30=1/1,2,3,16;
1/6=100,10=4,14=-1,18=20/3(1);
99//99;
2/9=110,15=1/2;
3/5=7,6=1,8=11,11=2,16=1,17=8,25=1,30=1/1,2,3;
4/5=5,11=1,16=2/1;
5/5=2,7=600,38=4,42=-5/2;
7/30=1/1,2,3,16;
1/6=100,14=-1,18=20/3(-5);
2/9=110,15=1/2;
6/7=2,8=2,9=2,10=2,19=2,28=1/1;
99/9=1/99;
-----------------------
UO2 ion DFT optimization
-----------------------
Symbolic Z-matrix:
Charge =  2 Multiplicity = 1
U                     0     0.          0.          0.
O                     0     2.02515     0.          Z1
O                     0    X1           0.          Z2
      Variables:
 Z1                    0.
 Z2                    0.
 X1                   -2.02515


GradGradGradGradGradGradGradGradGradGradGradGradGradGradGradGradGradGra
d
 Berny optimization.
 Initialization pass.
                          ----------------------------
```

```
                          !    Initial Parameters    !
                          ! (Angstroms and Degrees)  !
 -------------------------                            -----------------
-------
 ! Name  Definition              Value          Derivative Info.
!
 ---------------------------------------------------------------------
-------
 ! R1    R(1,2)                  2.0251         calculate D2E/DX2
analytical!
 ! R2    R(1,3)                  2.0251         calculate D2E/DX2
analytical!
 ! A1    L(2,1,3,-2,-1)         180.            calculate D2E/DX2
analytical!
 ! A2    L(2,1,3,-3,-2)         180.            calculate D2E/DX2
analytical!
 ---------------------------------------------------------------------
-------
 Trust Radius=3.00D-01 FncErr=1.00D-07 GrdErr=1.00D-06
 Number of steps in this run= 100 maximum allowed number of steps= 100.

GradGradGradGradGradGradGradGradGradGradGradGradGradGradGradGradGradGra
d

                         Input orientation:
 ---------------------------------------------------------------------
 Center     Atomic     Atomic              Coordinates (Angstroms)
 Number     Number      Type              X           Y           Z
 ---------------------------------------------------------------------
    1         92           0        0.000000    0.000000    0.000000
    2          8           0        2.025145    0.000000    0.000000
    3          8           0       -2.025145    0.000000    0.000000
 ---------------------------------------------------------------------
                    Distance matrix (angstroms):
                    1          2          3
     1  U    0.000000
     2  O    2.025145   0.000000
     3  O    2.025145   4.050290   0.000000
 Symmetry turned off by external request.
 Stoichiometry    O2U(2+)
 Framework group  D*H[O(U),C*(O.O)]
 Deg. of freedom    1
 Full point group                 D*H     NOp   8
 Rotational constants (GHZ):      0.0000000      3.8520604
3.8520604
 Isotopes: U-238,O-16,O-16
 General basis read from cards:  (5D, 7F)


=====================================================================
=============================================================
 Integral buffers will be    262144 words long.
 Raffenetti 2 integral format.
```

```
 Two-electron integral symmetry is turned off.
    77 basis functions      128 primitive gaussians
    12 alpha electrons       12 beta electrons
       nuclear repulsion energy        48.6024301045 Hartrees.
 One-electron integrals computed using PRISM.
   1 Symmetry operations used in ECPInt.
 ECPInt:  NShTT=      378 NPrTT=      677 LenC2=      378 LenP2D=      668.
 LDataN:  DoStor=F MaxTD1= 7 Len=  274
 LDataN:  DoStor=T MaxTD1= 7 Len=  274
 NBasis=    77 RedAO= T  NBF=    77
 NBsUse=    77 1.00D-04 NBFU=    77
 Projected Huckel Guess.
 Requested convergence on RMS density matrix=1.00D-08 within 600
cycles.
 Requested convergence on MAX density matrix=1.00D-06.
 Virtual orbitals will be shifted by   0.200 hartree.
 No pruned grid is available for atomic number  92.

 Restarting incremental Fock formation.
 SCF Done:  E(RB+HF-LYP) =  -82.7062193077     A.U. after  286 cycles
             Convg  =    0.7037D-08             -V/T =  2.7893
             S**2   =   0.0000
 Range of M.O.s used for correlation:     1    77
 NBasis=    77 NAE=    12 NBE=    12 NFC=     0 NFV=     0
 NROrb=     77 NOA=    12 NOB=    12 NVA=    65 NVB=    65

 **** Warning!!: The largest alpha MO coefficient is  0.10846328D+02

   1 Symmetry operations used in ECPInt.
 ECPInt:  NShTT=      378 NPrTT=      677 LenC2=      378 LenP2D=      668.
 LDataN:  DoStor=F MaxTD1= 8 Len=  415
 LDataN:  DoStor=T MaxTD1= 8 Len=  415
 G2DrvN: will do    3 atoms at a time, making    1 passes doing
MaxLOS=3.
 No pruned grid is available for atomic number  92.
 FoFDir used for L=0 through L=3.
          Differentiating once with respect to electric field.
                with respect to dipole field.
          Differentiating once with respect to nuclear coordinates.
 Symmetry not used in FoFDir.
 MinBra= 0 MaxBra= 3 Meth= 1.
 IRaf=       0 NMat=  12 IRICut=       12 DoRegI=T DoRafI=T ISym2E= 0
JSym2E=0.
 No pruned grid is available for atomic number  92.
          There are  12 degrees of freedom in the 1st order CPHF.
   9 vectors were produced by pass  0.
 AX will form   9 AO Fock derivatives at one time.
   9 vectors were produced by pass  1.
   9 vectors were produced by pass  2.
   9 vectors were produced by pass  3.
   9 vectors were produced by pass  4.
   9 vectors were produced by pass  5.
   6 vectors were produced by pass  6.
```

```
  4 vectors were produced by pass  7.
  4 vectors were produced by pass  8.
  1 vectors were produced by pass  9.
  1 vectors were produced by pass 10.
 Inv2:  IOpt= 1 Iter= 1 AM= 1.53D-14 Conv= 1.00D-12.
 Inverted reduced A of dimension  70 with in-core refinement.

 ********************************************************************

           Population analysis using the SCF density.

 ********************************************************************

 Alpha  occ. eigenvalues --   -2.42764  -1.56417  -1.49124  -1.49124  -
1.40656
 Alpha  occ. eigenvalues --   -1.27423  -0.84780  -0.83852  -0.83660  -
0.83660
 Alpha  occ. eigenvalues --   -0.82010  -0.82010
 Alpha virt. eigenvalues --   -0.71659  -0.71659  -0.68889  -0.68781  -
0.65436
 Alpha virt. eigenvalues --   -0.65436  -0.58388  -0.54728  -0.53328  -
0.53317
 Alpha virt. eigenvalues --   -0.43636  -0.43636  -0.35246  -0.35246  -
0.29309
 Alpha virt. eigenvalues --   -0.25262  -0.19691  -0.19691  -0.19050  -
0.19039
 Alpha virt. eigenvalues --   -0.17544  -0.13360  -0.13360  -0.09763  -
0.06829
 Alpha virt. eigenvalues --    0.15760   0.15760   0.15959   0.16017
0.22333
 Alpha virt. eigenvalues --    0.24839   0.25131   0.25131   0.25250
0.25287
 Alpha virt. eigenvalues --    0.28131   0.28131   0.37145   0.40470
0.40470
 Alpha virt. eigenvalues --    0.43680   0.43680   0.45713   0.47214
0.76136
 Alpha virt. eigenvalues --    0.76242   1.42165   1.42166   1.46435
1.46438
 Alpha virt. eigenvalues --    1.49290   1.49290   1.65971   1.77219
1.77220
 Alpha virt. eigenvalues --    1.96823   4.05441   4.05441   4.12989
4.12989
 Alpha virt. eigenvalues --    4.26518   4.28941  26.80282  29.46744
32.42515
          Condensed to atoms (all electrons):
               1          2          3
  1  U   11.105692   0.347243   0.347243
  2  O    0.347243   5.751585   0.001082
  3  O    0.347243   0.001082   5.751586
 Total atomic charges:
               1
  1  U    2.199822
  2  O   -0.099910
```

```
 3  O   -0.099911
Sum of Mulliken charges=   2.00000
Atomic charges with hydrogens summed into heavy atoms:
                1
 1  U    2.199822
 2  O   -0.099910
 3  O   -0.099911
Sum of Mulliken charges=   2.00000
Electronic spatial extent (au):  <R**2>=   242.7517
Charge=     2.0000 electrons
Dipole moment (Debye):
   X=     0.0000    Y=     0.0000    Z=     0.0000  Tot=     0.0000
Quadrupole moment (Debye-Ang):
  XX=   -34.7912   YY=   -27.6657   ZZ=   -27.6657
  XY=     0.0000   XZ=     0.0000   YZ=     0.0000
Octapole moment (Debye-Ang**2):
 XXX=     0.0000  YYY=     0.0000  ZZZ=     0.0000  XYY=     0.0000
 XXY=     0.0000  XXZ=     0.0000  XZZ=     0.0000  YZZ=     0.0000
 YYZ=     0.0000  XYZ=     0.0000
Hexadecapole moment (Debye-Ang**3):
XXXX=  -272.3735 YYYY=   -23.1409 ZZZZ=   -23.1409 XXXY=     0.0004
XXXZ=     0.0001 YYYX=     0.0000 YYYZ=     0.0000 ZZZX=     0.0000
ZZZY=     0.0000 XXYY=   -52.3939 XXZZ=   -52.3940 YYZZ=    -7.7175
XXYZ=     0.0001 YYXZ=     0.0000 ZZXY=     0.0000
N-N= 4.860243010451D+01 E-N=-2.723551435011D+02  KE=
4.622358782844D+01
 Exact polarizability:  66.383   0.000  16.895   0.000   0.000  16.895
Approx polarizability: 299.712   0.000  27.280   0.000   0.000  27.280
  1 Symmetry operations used in ECPInt.
ECPInt:  NShTT=     378 NPrTT=     677 LenC2=     378 LenP2D=     668.
LDataN:  DoStor=F MaxTD1= 9 Len=  602
LDataN:  DoStor=T MaxTD1= 9 Len=  602
No pruned grid is available for atomic number  92.
---------------------------------------------------------------------
Center     Atomic                   Forces (Hartrees/Bohr)
Number     Number              X              Y              Z
---------------------------------------------------------------------
   1         92           0.000000152    0.000000000    0.000000000
   2          8          -0.168012331   -0.000000008   -0.000000003
   3          8           0.168012179    0.000000007    0.000000002
---------------------------------------------------------------------
Cartesian Forces:  Max     0.168012331 RMS     0.079201737


GradGradGradGradGradGradGradGradGradGradGradGradGradGradGradGradGradGra
d
 Berny optimization.
 Internal  Forces:  Max     0.168012331 RMS     0.118802605
 Search for a local minimum.
 Step number   1 out of a maximum of 100
 All quantities printed in internal units (Hartrees-Bohrs-Radians)
 Second derivative matrix not updated -- analytic derivatives used.
 The second derivative matrix:
```

```
                       R1        R2        A1        A2
            R1       0.06744
            R2      -0.02273   0.06743
            A1       0.00000   0.00000   0.09820
            A2       0.00000   0.00000   0.00000   0.09820
     Eigenvalues ---    0.04470   0.09016   0.09820   0.09820
 RFO step:  Lambda=-2.16302376D-01.
 Linear search not attempted -- first point.
 Maximum step size (   0.300) exceeded in Quadratic search.
    -- Step size scaled by   0.330
 Iteration  1 RMS(Cart)=  0.14142136 RMS(Int)=  0.00857864
 Iteration  2 RMS(Cart)=  0.00857864 RMS(Int)=  0.00000000
 SLEqS1 Cycle:     91 Max:0.234561E-13 RMS:0.122675E-13 Conv:0.298874E-
14
 SLEqS1 Cycle:     91 Max:0.142515E-12 RMS:0.745350E-13 Conv:0.298874E-
14
 Iteration  3 RMS(Cart)=  0.00000001 RMS(Int)=  0.00000000
 Variable       Old X    -DE/DX   Delta X   Delta X   Delta X     New X
                                  (Linear)    (Quad)   (Total)
    R1         3.82697  -0.16801   0.00000  -0.21213  -0.21213   3.61484
    R2         3.82697  -0.16801   0.00000  -0.21213  -0.21213   3.61484
    A1         3.14159   0.00000   0.00000   0.00000   0.00000   3.14159
    A2         3.14159   0.00000   0.00000   0.00000   0.00000   3.14159
         Item               Value     Threshold  Converged?
 Maximum Force            0.168012     0.000450     NO
 RMS     Force            0.118803     0.000300     NO
 Maximum Displacement     0.212132     0.001800     NO
 RMS     Displacement     0.150000     0.001200     NO
 Predicted change in Energy=-2.011667D-03

GradGradGradGradGradGradGradGradGradGradGradGradGradGradGradGradGradGra
d

                          Input orientation:
 ---------------------------------------------------------------------
 Center     Atomic     Atomic              Coordinates (Angstroms)
 Number     Number      Type              X           Y           Z
 ---------------------------------------------------------------------
    1         92           0       -0.000001   -0.000001   -0.000001
    2          8           0        1.754137    0.000000    0.000000
    3          8           0       -1.754136    0.000000    0.000000
 ---------------------------------------------------------------------
                    Distance matrix (angstroms):
                         1          2          3
     1  U    0.000000
     2  O    1.754137   0.000000
     3  O    1.754135   3.508273   0.000000
 Symmetry turned off by external request.
 Error permuting atoms in Fill, LPerm:
   0   0   0
 Symmetry turned off:
 Internal error in symmetry package.
```

```
 Rotational constants (GHZ):***************      5.1342690
5.1342690
 Isotopes: U-238,O-16,O-16
 Basis read from rwf:  (5D, 7F)
 Pseudo-potential data read from read-write file.
 Integral buffers will be    262144 words long.
 Raffenetti 2 integral format.
 Two-electron integral symmetry is turned off.
    77 basis functions      128 primitive gaussians
    12 alpha electrons       12 beta electrons
       nuclear repulsion energy        56.1113545651 Hartrees.
 One-electron integrals computed using PRISM.
   1 Symmetry operations used in ECPInt.
 ECPInt:  NShTT=     378 NPrTT=     677 LenC2=     378 LenP2D=     668.
 LDataN:  DoStor=F MaxTD1= 7 Len=  274
 LDataN:  DoStor=T MaxTD1= 7 Len=  274
 NBasis=    77 RedAO= T  NBF=    77
 NBsUse=    77 1.00D-04 NBFU=    77
 Initial guess read from the read-write file:
 Requested convergence on RMS density matrix=1.00D-08 within 600
cycles.
 Requested convergence on MAX density matrix=1.00D-06.
 Virtual orbitals will be shifted by   0.200 hartree.
 No pruned grid is available for atomic number  92.
 Restarting incremental Fock formation.
 SCF Done:  E(RB+HF-LYP) =  -82.8430333772     A.U. after   20 cycles
             Convg  =    0.3393D-08             -V/T =  2.7665
             S**2   =   0.0000
   1 Symmetry operations used in ECPInt.
 ECPInt:  NShTT=     378 NPrTT=     677 LenC2=     378 LenP2D=     668.
 LDataN:  DoStor=F MaxTD1= 8 Len=  415
 LDataN:  DoStor=T MaxTD1= 8 Len=  415
 No pruned grid is available for atomic number  92.
 ---------------------------------------------------------------------
 Center     Atomic                     Forces (Hartrees/Bohr)
 Number     Number              X              Y              Z
 ---------------------------------------------------------------------
    1         92           0.000001883    0.000000120    0.000000149
    2          8          -0.067479103   -0.000000060   -0.000000075
    3          8           0.067477221   -0.000000060   -0.000000075
 ---------------------------------------------------------------------
 Cartesian Forces:  Max     0.067479103 RMS     0.031809511


GradGradGradGradGradGradGradGradGradGradGradGradGradGradGradGradGradGra
d
 Berny optimization.
 Internal  Forces:  Max     0.067479103 RMS     0.047714266
 Search for a local minimum.
 Step number   3 out of a maximum of 100
 All quantities printed in internal units (Hartrees-Bohrs-Radians)
 Update second derivatives using information from points  2  3
 The second derivative matrix:
```

```
                       R1        R2        A1        A2
            R1       0.17992
            R2       0.08976   0.17993
            A1       0.00000   0.00000   0.09820
            A2       0.00000   0.00000   0.00000   0.09820
     Eigenvalues ---    0.09016   0.09820   0.09820   0.26968
 RFO step:  Lambda= 0.00000000D+00.
 Quartic linear search produced a step of  0.44627.
 Iteration  1 RMS(Cart)=  0.09466882 RMS(Int)=  0.00000005
 SLEqS1 Cycle:     91 Max:0.503364E-10 RMS:0.233395E-10 Conv:0.442720E-
13
 SLEqS1 Cycle:     91 Max:0.192216E-11 RMS:0.100529E-11 Conv:0.442720E-
13
 Iteration  2 RMS(Cart)=  0.00000006 RMS(Int)=  0.00000000
 Variable       Old X    -DE/DX   Delta X   Delta X   Delta X     New X
                                  (Linear)    (Quad)   (Total)
    R1        3.31484  -0.06748  -0.13388  -0.00002  -0.13390   3.18094
    R2        3.31484  -0.06748  -0.13388   0.00002  -0.13387   3.18097
    A1        3.14159   0.00000   0.00000   0.00000   0.00000   3.14159
    A2        3.14159   0.00000   0.00000   0.00000   0.00000   3.14159
         Item               Value     Threshold  Converged?
 Maximum Force            0.067479     0.000450     NO
 RMS     Force            0.047714     0.000300     NO
 Maximum Displacement     0.133887     0.001800     NO
 RMS     Displacement     0.094669     0.001200     NO
 Predicted change in Energy=-4.833913D-03


GradGradGradGradGradGradGradGradGradGradGradGradGradGradGradGradGradGra
d

                          Input orientation:
 ---------------------------------------------------------------------
 Center     Atomic     Atomic              Coordinates (Angstroms)
 Number     Number      Type              X           Y           Z
 ---------------------------------------------------------------------
    1         92           0       -0.000029    0.000000    0.000000
    2          8           0        1.686750    0.000000    0.000000
    3          8           0       -1.686722    0.000000    0.000000
 ---------------------------------------------------------------------
                    Distance matrix (angstroms):
                    1          2          3
     1  U    0.000000
     2  O    1.686779   0.000000
     3  O    1.686693   3.373472   0.000000
 Symmetry turned off by external request.
 Error permuting atoms in Fill, LPerm:
   0   0   0
 Symmetry turned off:
 Internal error in symmetry package.
 Rotational constants (GHZ):***************      5.5527882
5.5527882
 Isotopes: U-238,O-16,O-16
```

```
 Basis read from rwf:  (5D, 7F)
 Pseudo-potential data read from read-write file.
 Integral buffers will be    262144 words long.
 Raffenetti 2 integral format.
 Two-electron integral symmetry is turned off.
    77 basis functions      128 primitive gaussians
    12 alpha electrons       12 beta electrons
       nuclear repulsion energy        58.3535119587 Hartrees.
 One-electron integrals computed using PRISM.
   1 Symmetry operations used in ECPInt.
 ECPInt:  NShTT=      378 NPrTT=      677 LenC2=      378 LenP2D=      668.
 LDataN:  DoStor=F MaxTD1= 7 Len=  274
 LDataN:  DoStor=T MaxTD1= 7 Len=  274
 NBasis=    77 RedAO= T  NBF=    77
 NBsUse=    77 1.00D-04 NBFU=    77
 Initial guess read from the read-write file:
 Requested convergence on RMS density matrix=1.00D-08 within 600
cycles.
 Requested convergence on MAX density matrix=1.00D-06.
 Virtual orbitals will be shifted by   0.200 hartree.
 No pruned grid is available for atomic number  92.
 SCF Done:  E(RB+HF-LYP) =  -82.8522079967     A.U. after   11 cycles
             Convg  =    0.7848D-08             -V/T =  2.7494
             S**2   =   0.0000
   1 Symmetry operations used in ECPInt.
 ECPInt:  NShTT=      378 NPrTT=      677 LenC2=      378 LenP2D=      668.
 LDataN:  DoStor=F MaxTD1= 8 Len=  415
 LDataN:  DoStor=T MaxTD1= 8 Len=  415
 No pruned grid is available for atomic number  92.
 ---------------------------------------------------------------------
 Center     Atomic                     Forces (Hartrees/Bohr)
 Number     Number              X              Y              Z
 ---------------------------------------------------------------------
    1         92          0.000110780   -0.000000005   -0.000000007
    2          8         -0.000075154    0.000000003    0.000000003
    3          8         -0.000035626    0.000000003    0.000000003
 ---------------------------------------------------------------------
 Cartesian Forces:  Max     0.000110780 RMS     0.000046175


GradGradGradGradGradGradGradGradGradGradGradGradGradGradGradGradGradGra
d
 Berny optimization.
 Internal  Forces:  Max     0.000075154 RMS     0.000041585
 Search for a local minimum.
 Step number   5 out of a maximum of 100
 All quantities printed in internal units (Hartrees-Bohrs-Radians)
 Update second derivatives using information from points  3  4  5
 Trust test= 1.20D+00 RLast= 9.21D-03 DXMaxT set to 5.68D-01
 The second derivative matrix:
                          R1        R2        A1        A2
          R1           0.37858
          R2           0.27969   0.36142
```

```
          A1           0.00000   0.00000   0.09820
          A2           0.00000   0.00000   0.00000   0.09820
     Eigenvalues ---    0.09018   0.09820   0.09820   0.64982
 RFO step:  Lambda=-6.72880839D-08.
 Quartic linear search produced a step of -0.00491.
 Iteration  1 RMS(Cart)=  0.00025003 RMS(Int)=  0.00000001
 SLEqS1 Cycle:    91 Max:0.134361E-12 RMS:0.636985E-13 Conv:0.732943E-
14
 Iteration  2 RMS(Cart)=  0.00000000 RMS(Int)=  0.00000001
 Variable       Old X    -DE/DX   Delta X   Delta X   Delta X     New X
                                  (Linear)    (Quad)   (Total)
    R1         3.18755  -0.00008  -0.00003  -0.00060  -0.00063   3.18692
    R2         3.18739   0.00004  -0.00003   0.00062   0.00059   3.18798
    A1         3.14159   0.00000   0.00000   0.00000   0.00000   3.14159
    A2         3.14159   0.00000   0.00000   0.00000   0.00000   3.14159
         Item               Value     Threshold  Converged?
 Maximum Force            0.000075     0.000450     YES
 RMS     Force            0.000042     0.000300     YES
 Maximum Displacement     0.000407     0.001800     YES
 RMS     Displacement     0.000250     0.001200     YES
 Predicted change in Energy=-3.430837D-08
 Optimization completed.
    -- Stationary point found.
                          ----------------------------
                          !   Optimized Parameters   !
                          ! (Angstroms and Degrees)  !
 -------------------------                            ------------------
-------
 ! Name  Definition              Value          Derivative Info.
!
 ---------------------------------------------------------------------
-------
 ! R1    R(1,2)                  1.6868         -DE/DX =   -0.0001
!
 ! R2    R(1,3)                  1.6867         -DE/DX =    0.
!
 ! A1    L(2,1,3,-2,-1)        180.             -DE/DX =    0.
!
 ! A2    L(2,1,3,-3,-2)        180.             -DE/DX =    0.
!
 ---------------------------------------------------------------------
-------

GradGradGradGradGradGradGradGradGradGradGradGradGradGradGradGradGradGra
d

                         Input orientation:
 ---------------------------------------------------------------------
 Center     Atomic      Atomic             Coordinates (Angstroms)
 Number     Number       Type              X           Y           Z
 ---------------------------------------------------------------------
    1         92             0       -0.000029    0.000000    0.000000
    2          8             0        1.686750    0.000000    0.000000
```

```
   3          8             0       -1.686722    0.000000    0.000000
---------------------------------------------------------------------
                    Distance matrix (angstroms):
                    1          2          3
    1  U    0.000000
    2  O    1.686779   0.000000
    3  O    1.686693   3.373472   0.000000
 Symmetry turned off by external request.
 Error permuting atoms in Fill, LPerm:
   0   0   0
 Symmetry turned off:
 Internal error in symmetry package.
 Rotational constants (GHZ):***************      5.5527882
5.5527882
 Isotopes: U-238,O-16,O-16

 ********************************************************************

            Population analysis using the SCF density.

 ********************************************************************

 Alpha  occ. eigenvalues --   -2.43498  -1.75890  -1.47737  -1.47737  -
1.47559
 Alpha  occ. eigenvalues --   -1.19119  -0.92485  -0.92485  -0.92218  -
0.92218
 Alpha  occ. eigenvalues --   -0.91194  -0.89540
 Alpha virt. eigenvalues --   -0.68664  -0.68664  -0.67841  -0.67837  -
0.58663
 Alpha virt. eigenvalues --   -0.58663  -0.53135  -0.51767  -0.51762  -
0.37287
 Alpha virt. eigenvalues --   -0.34398  -0.34398  -0.34322  -0.34322  -
0.29355
 Alpha virt. eigenvalues --   -0.24002  -0.20488  -0.20488  -0.18422  -
0.18420
 Alpha virt. eigenvalues --   -0.17346  -0.12805  -0.12453  -0.12453
0.04439
 Alpha virt. eigenvalues --    0.15131   0.15152   0.17377   0.17377
0.24172
 Alpha virt. eigenvalues --    0.25831   0.25831   0.26709   0.26752
0.29425
 Alpha virt. eigenvalues --    0.29806   0.29806   0.39982   0.40244
0.45020
 Alpha virt. eigenvalues --    0.45020   0.45386   0.45386   0.60906
0.75632
 Alpha virt. eigenvalues --    0.78802   1.35267   1.35267   1.48368
1.48371
 Alpha virt. eigenvalues --    1.55566   1.55566   1.87596   1.87596
2.00725
 Alpha virt. eigenvalues --    2.37266   4.03314   4.03314   4.12033
4.12033
 Alpha virt. eigenvalues --    4.27938   4.35129  26.99418  32.15281
35.82324
```

```
          Condensed to atoms (all electrons):
                1          2          3
 1  U   11.217815   0.323842   0.323885
 2  O    0.323842   5.734565   0.008859
 3  O    0.323885   0.008859   5.734448
Total atomic charges:
                1
 1  U    2.134458
 2  O   -0.067266
 3  O   -0.067192
Sum of Mulliken charges=   2.00000
Atomic charges with hydrogens summed into heavy atoms:
                1
 1  U    2.134458
 2  O   -0.067266
 3  O   -0.067192
Sum of Mulliken charges=   2.00000
Electronic spatial extent (au):  <R**2>=   186.5152
Charge=     2.0000 electrons
Dipole moment (Debye):
   X=    -0.0007    Y=     0.0000    Z=     0.0000  Tot=     0.0007
Quadrupole moment (Debye-Ang):
  XX=   -32.5108   YY=   -27.1867   ZZ=   -27.1867
  XY=     0.0000   XZ=     0.0000   YZ=     0.0000
Octapole moment (Debye-Ang**2):
 XXX=    -0.0001  YYY=     0.0000  ZZZ=     0.0000  XYY=     0.0000
 XXY=     0.0000  XXZ=     0.0000  XZZ=     0.0000  YZZ=     0.0000
 YYZ=     0.0000  XYZ=     0.0000
Hexadecapole moment (Debye-Ang**3):
XXXX=  -191.4618 YYYY=   -22.0209 ZZZZ=   -22.0209 XXXY=     0.0000
XXXZ=     0.0000 YYYX=     0.0000 YYYZ=     0.0000 ZZZX=     0.0000
ZZZY=     0.0000 XXYY=   -37.0227 XXZZ=   -37.0227 YYZZ=    -7.3404
XXYZ=     0.0000 YYXZ=     0.0000 ZZXY=     0.0000
N-N= 5.835351195867D+01 E-N=-2.917631800479D+02  KE=
4.736082042513D+01
Atom   2 needs constant  BL=   2.0251450000 but is    2.6356093122
Input z-matrix variables are not compatible with final structure.
PRSFWG-- UNABLE TO FIND LEFT SQUARE BRACKET.
NUMDOF-- UNRECOGNIZED SYMMETRIC SUBSPACE, ICHAR= E   "
1|1|UNPC-UNK|FOpt|RB3LYP|Gen|  |PCUSER|03-Mar-2003|0||# B3LYP/GEN 5D,7F
 PSEUDO=READ NOSYMM SCF=(MAXCYC=600) OPT=(CALCFC,REDUNDANT,MAXCYC=100)
 GEOM=CONNECTIVITY||UO2 ion DFT optimization||2,1|U,-0.0000288321,0.00
0000071,0.0000000886|O,1.6867503993,-0.0000000355,-0.0000000443|O,-1.6
867215672,-0.0000000355,-0.0000000443||Version=x86-Win32-G98RevA.9|HF=
-82.852208|RMSD=7.848e-009|RMSF=4.618e-005|Dipole=-0.0002365,0.0000003
,0.0000003|PG=||@


SIC AS THE CAWSE OF EWERY THING IS, SIC WILBE THE EFFECT.
-- PROVERBS AND REASONS OF THE YEAR 1585
          AS REPRINTED IN PAISLEY MAGAZINE 1828.
Job cpu time:  0 days  2 hours 43 minutes 54.0 seconds.
```

```
 File lengths (MBytes):  RWF=     19 Int=      0 D2E=      0 Chk=     11 Scr=
1
 Normal termination of Gaussian 98.
```